

The thermal stability and non-isothermal decomposition kinetics of a zinc ferrite precursor

Oana Carp ^{a,*}, E. Segal ^b, Luminița Patron ^a, Ruxandra Birjega ^c, C. Craiu ^c and N. Stănică ^a

^a *Institute of Physical Chemistry, Splaiul Independentei, Nr.202, sector 6, Bucharest (Romania)*

^b *Department of Physical Chemistry, Faculty of Chemistry, University of Bucharest, Bulevardul Carol I, Nr. 13, Bucharest (Romania)*

^c *Zecasin S.A., Chemical Research & Development & Production, Splaiul Independentei, Nr. 202, sector 6, Bucharest (Romania)*

(Received 23 November 1992; accepted 16 December 1992)

Abstract

The authors present the results obtained from an investigation of the thermal stability and decomposition kinetics of the polynuclear coordination compound $[\text{Fe(II)Fe(II)-Zn(II)(C}_2\text{O}_4)_2(\text{OH})_3] \cdot 4\text{H}_2\text{O}$, a precursor of zinc ferrite. The non-isothermal kinetics parameters over various significant ranges of conversion were evaluated.

INTRODUCTION

Following our research concerning the possibilities of obtaining mixed oxides by the thermal decomposition of polynuclear coordination compounds as precursors [1–6], this paper deals with the thermal stability and non-isothermal decomposition kinetics of a polynuclear coordination compound containing the oxalate anion. This anion was chosen because of its relatively high volatility. This results in the precursor having a fairly low thermal stability: it undergoes total decomposition at temperatures below 500°C.

EXPERIMENTAL

The coordination compound of molecular formula $[\text{Fe(II)Fe(III)Zn(II)-(C}_2\text{O}_4)_2(\text{OH})_3] \cdot 4\text{H}_2\text{O}$ was synthesized according to a method described elsewhere [7].

The heating curves were recorded using a MOM-Budapest Q-1500

* Corresponding author.

derivatograph, type Paulik–Paulik–Erdey, in a static air atmosphere at various heating rates in the range $0.6\text{--}10\text{ K min}^{-1}$ and with $\alpha\text{-Al}_2\text{O}_3$ as an inert material.

The evolved gases were analysed using a Hewlett-Packard GC-MS 5595 mass spectrometer, coupled with a micro-reactor.

Measurements of magnetic susceptibility and saturation magnetization were performed with a magnetic balance, the standard being HgCo(SCN) .

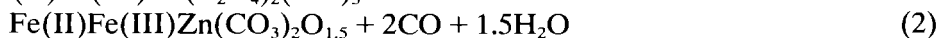
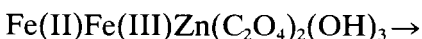
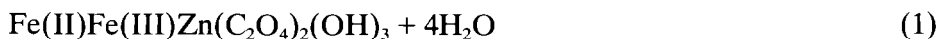
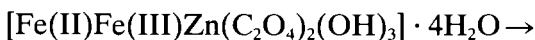
The crystalline states of the compounds and the decomposition products, were investigated using a DRON 3 X-ray diffractometer with $\text{Co K}\alpha$ radiation.

To analyse the thermogravimetric data, two programs written in BASIC, namely DISCRIM 1 (D1) [8] and DISCRIM 2 (D2) were run on a TIM-S computer. Both programs can discriminate among various decomposition mechanisms, indicating the most probable conversion function $f(\alpha)$. The criterion for the most probable mechanism is the mean square deviation of the calculated $f(\alpha)$ values from the experimental values. For DISCRIM 2, the mean square deviations are displayed.

Taking into account the possibility of the mechanism changing with the degree of conversion as well as the overall (α, T) curve, the kinetic parameters were evaluated for particular ranges of conversion degree. The intervals $0 < \alpha < \alpha_{ip}$ and $\alpha_{ip} < \alpha < 1$, where the subscript ip indicates the inflection of the TG curve, were considered. For those TG curves with an obvious induction period, the non-isothermal parameters were also evaluated.

RESULTS AND DISCUSSION

From the thermogravimetric data, it can be concluded that the compound $[\text{Fe(II)Fe(II)(Zn(II)(C}_2\text{O}_4)_2(\text{OH})_3] \cdot 4\text{H}_2\text{O}$ decomposes to an oxide phase, according to the sequence



As shown by its X-ray powder diffractogram, $[\text{Fe(II)Fe(III)Zn(C}_2\text{O}_4)_2(\text{OH})_3] \cdot 4\text{H}_2\text{O}$ has a crystalline structure. Table 1 lists the values of the interplanar distances d corresponding to the diffraction lines and their relative intensity. The mean crystallite size for the most intense line, calculated using Sherrer's formula [10], is $d = 217\text{ \AA}$.

The magnetic and X-ray diffraction data indicated that the final solid reaction product is not Fe_2ZnO_4 alone. The magnetic moment, evaluated

TABLE 1

X-ray powder diffraction data of the compound $[\text{Fe(II)Fe(III)Zn}(\text{C}_2\text{O}_4)(\text{OH})_2] \cdot 4\text{H}_2\text{O}$

Line	$d/\text{\AA}$	Relative intensity	Line	$d/\text{\AA}$	Relative intensity
1	4.759	100	14	2.158	4
2	4.655	96	15	2.107	4
3	3.905	23	16	2.094	8
4	3.673	10	17	2.080	5
5	3.555	30	18	2.030	8
6	2.949	50	19	1.988	6
7	2.704	28	20	1.955	2
8	2.649	11	21	1.941	4
9	2.628	21	22	1.928	5
10	2.557	10.5	23	1.922	7
11	2.512	19	24	1.881	14
12	2.229	9.5	25	1.839	10
13	2.208	10	26	1.798	8

from magnetic susceptibility, has a non-zero value ($\mu = 0.93 \text{ BM}$), due to the presence of the ferrimagnetic oxide Fe_2O_4 .

The mass spectra of the evolved gases showed the presence of water evolved in reaction (1), of carbon monoxide and water evolved in reaction (2), and of carbon dioxide evolved in reaction (3).

The calculated total weight loss from reactions (1), (2) and (3) is 49.40%, while the experimental value is 48.64%.

Table 2 lists the non-isothermal kinetic parameters corresponding to the most probable mechanism for all the (α, T) curve.

For each reaction, the value of the rate constant, calculated from the pre-exponential factor A and activation energy E values according to the Arrhenius equation at a temperature in the range of its occurrence, is also given in Table 2.

Table 3 lists the values of the non-isothermal kinetics parameters for the selected ranges of conversion.

As shown in Table 2, for reaction (1) both programs D1 and D2 lead to similar values for the non-isothermal kinetic parameters. These are characteristic for a contracting sphere mechanism. In practise, the values of the non-isothermal kinetic parameters do not depend on the heating rate, thus showing no heat transfer limitations. Nor do the rate constants $k_{433 \text{ K}}$ change significantly with the heating rate. The contracting sphere mechanism is also indicated for $0 < \alpha < \alpha_{\text{ip}}$ for $\alpha_{\text{ip}} < \alpha < 1$, and for the acceleratory period, with practically the same values of the non-isothermal kinetic parameters as shown in Table 3. Thus for reaction (1), the same kinetic parameter values were obtained over the whole range of conversion, as

TABLE 2
 Non-isothermal kinetic parameter values for the range $0 < \alpha < 1$

$\beta/K \text{ min}^{-1}$	$T_1^a - T_f$ in $^{\circ}\text{C}$	T_{max}^b in $^{\circ}\text{C}$	Computation program	$f(\alpha)$	A/s^{-1}	$E/\text{kcal mol}^{-1}$	$k \times 10^3/s^{-1}$	Mean square deviation
Reaction (1): the rate constant k is calculated for $T = 433 \text{ K}$								
10	128.5–219.5	199	DISCRIM 2	Contracting sphere ($1 - \alpha$) $n = 0.69$	2.03×10^8	19.42	39.9	10.21
			DISCRIM 1		5.75×10^8	19.53	74.1	1.01
5	124–205	182	DISCRIM 2	Contracting sphere ($1 - \alpha$) $n = 0.67$	1.91×10^8	18.69	66.6	12.36
			DISCRIM 1		3.02×10^8	18.95	78.9	5.85
2.5	120–193	173	DISCRIM 2	Contracting sphere ($1 - \alpha$) $n = 0.71$	4.43×10^8	18.82	115.8	7.32
			DISCRIM 1		7.70×10^8	19.40	109.4	4.80
1.25	119–174.5	155	DISCRIM 2	Contracting sphere ($1 - \alpha$) $n = 0.68$	1.76×10^8	19.00	41.9	6.31
			DISCRIM 1		8.27×10^8	19.78	79.3	4.78
0.6	117–166	149.5	DISCRIM 2	Contracting sphere ($1 - \alpha$) $n = 0.71$	5.13×10^8	19.47	51.2	6.07
			DISCRIM 1		4.33×10^9	21.32	68.9	1.69

Reaction (2): the rate constant k is calculated for $T = 533$ K

10	219.5–302.5	248.5	DISCRIM 2	Contracting sphere ($1 - \alpha$) $n = 0.68$	5.61×10^7	21.31	43.5	1.92
			DISCRIM 1		2.80×10^7	20.35	55.9	0.71
5	205–295	260	DISCRIM 2	Contracting sphere ($1 - \alpha$) $n = 0.62$	1.23×10^6	17.40	44.8	0.17
			DISCRIM 1		5.53×10^5	17.25	23.2	2.90
2.5	193–273	249	DISCRIM 2	Contracting sphere ($1 - \alpha$) $n = 0.69$	5.67×10^6	18.41	76.5	3.92
			DISCRIM 1		1.32×10^6	17.64	37.9	1.3
1.25	174.5–269	254.5	DISCRIM 2	Contracting sphere	7.50×10^5	17.47	25.5	6.11
			DISCRIM 1		–	–	–	–
0.6	166–258	236	DISCRIM 2	Contracting sphere ($1 - \alpha$) $n = 0.64$	3.38×10^5	16.00	47.4	5.92
			DISCRIM 1		7.41×10^4	14.39	88.9	2.75

Reaction (3): the rate constant k is calculated for $T = 588$ K

10	302–278		DISCRIM 2	Contracting cylinder	1.32×10	4.80	210.7	7.72
			DISCRIM 1	Contracting sphere	1.12×10^3	9.77	254.3	8.80
					–	–	–	–

TABLE 2 (continued)

$\beta/\text{K min}^{-1}$	$T_i^a - T_f$ in $^{\circ}\text{C}$	T_{max}^b in $^{\circ}\text{C}$	Computation program	$f(\alpha)$	A/s^{-1}	$E/\text{kcal mol}^{-1}$	$k \times 10^3/\text{s}^{-1}$	Mean square deviation
5	295–366		DISCRIM 2	Contracting cylinder	3.56×10	6.80	103.5	10.8
			DISCRIM 1	Contracting sphere	4.73×10^3	12.40	112.2	12.58
2.5	273–362		DISCRIM 2	Contracting cylinder	1.68×10	4.09	50.1	4.40
			DISCRIM 1	Contracting sphere	2.45×10^2	9.61	63.8	5.32
1.25	269–340		DISCRIM 2	Contracting cylinder	2.81×10	5.22	31.7	4.03
			DISCRIM 1	Contracting sphere	3.24×10^2	10.43	41.7	7.24
0.6	255–320		DISCRIM 2	Contracting cylinder	1.70×10	4.81	27.31	4.30
			DISCRIM 1	Contracting sphere	1.43×10^2	10.32	20.24	4.72

^a T_i and T_f are the initial and final temperatures.

^b T_{max} corresponds to the maximum reaction rate temperature.

TABLE 3

Non-isothermal kinetic parameters for various portions of the (α, \dot{T}) curve

Reaction	Conversion range	$\beta/K \text{ min}^{-1}$	$T_f - T_i$ in $^{\circ}\text{C}$	$f(\alpha)$	A/s^{-1}	$E/\text{kcal mol}^{-1}$	Mean square deviation
(1)							
	$\frac{0-\alpha_{ip}}{0-0.6973}$	10	128.5–191	Contracting sphere	0.82×10^8	17.21	10.71
	0–0.6606	5	124–182	Contracting sphere	3.15×10^8	19.08	12.29
	0–0.7020	2.5	120–173	Contracting sphere	1.89×10^8	18.74	1.15
	0–0.6250	1.25	119–155	Contracting sphere	1.54×10^8	18.46	3.28
	0–0.6463	0.6	117–149.5	Contracting sphere	3.34×10^8	19.03	1.86
	$\frac{\alpha_{ip}-1}{0.6973-1}$	10	191–219.5	Contracting sphere	3.07×10^8	19.95	0.20
	0.6606–1	5	182.5–205	Contracting sphere	1.05×10^8	18.58	0.34
	0.7020–1	2.5	173–193	Contracting sphere	3.22×10^8	19.20	7.32
	0.6250–1	1.25	155–174.5	Contracting sphere	3.15×10^8	19.67	13.52
	0.6431–1	0.6	149.5–16	Contracting sphere	9.38×10^8	18.73	9.3

TABLE 3 (continued)

Reaction	Conversion range	$\beta/K \text{ min}^{-1}$	$T_r - T_i$ in $^{\circ}\text{C}$	$f(\alpha)$	A/s^{-1}	$E/\text{kcal mol}^{-1}$	Mean square deviation
	Induction period						
	0-0.1517	10	128.5-161	Power law $(1/n)\alpha^{n-1}$ $n = 3/2$	4.77×10^{17}	40.58	12.8
	0-0.1928	5	124-156	Power law $(1/n)\alpha^{n-1}$ $n = 3/2$	2.71×10^{16}	37.5	8.40
	0-0.1048	2.5	120-138	Power law $(1/n)\alpha^{n-1}$ $n = 3/2$	1.62×10^{16}	34.33	2.31
	0-0.1114	1.25	119-132.5	Power law $(1/n)\alpha^{n-1}$ $n = 3/2$	4.54×10^{16}	39.82	16.21
	0-0.1290	0.6	177-128.5	Power law $(1/n)\alpha^{n-1}$ $n = 3/2$	6.12×10^{13}	30.42	5.05
	Acceleratory period						
	0.1517-0.6973	10	161-199	Contracting sphere	0.92×10^7	18.05	6.66
	0.1928-0.6606	5	156-182	Contracting sphere	1.48×10^8	18.85	1.75
	0.1040-0.7020	2.5	138-173	Contracting sphere	3.77×10^8	19.31	0.56

0.1114–0.6250	1.25	132.5–157.5	Contracting sphere	2.70×10^8	18.96	2.87
0.1280–0.6431	0.6	117–149.5	Contracting sphere	5.32×10^8	19.51	6.88
$\frac{0-\alpha_{ip}}{0-0.6867}$	10	295.5–248.5	Contracting sphere	1.82×10^6	15.93	0.50
0–0.6742	5	205–60	Contracting sphere	3.05×10^6	15.45	0.08
0–0.6500	2.5	193–249	Contracting sphere	1.27×10^6	16.25	6.31
0–0.6540	1.25	174.5–254.5	Contracting sphere	1.56×10^6	15.76	5.65
0–0.6371	0.6	166–236	Contracting sphere	4.13×10^4	14.70	5.35
$\frac{\alpha_{ip}-1}{0.6867-1}$	10	284.5–302.5	Contracting cylinder	5.08×10^7	19.78	1.71
0.6742–1	5	260–295	Contracting cylinder	1.64×10^7	19.00	5.95
0.6500–1	2.5	249–273	Contracting cylinder	1.94×10^7	21.11	3.85
0.6540–1	1.25	254.5–269	Contracting cylinder	8.84×10^6	20.13	5.52
0.6371–1	0.6	236–258	Contracting cylinder	6.24×10^6	19.85	3.72

(2)

well as for partial specified ranges, showing no change in reaction mechanism with conversion. Nevertheless, as shown in Table 3, one can detect an induction period described by a power law, $\alpha^n = kt$ with $n = 3/2$.

For reaction (2), the data listed in Table 2 also indicate a contracting sphere mechanism, as obtained using programs D1 and D2. A compensated slight change in the non-isothermal kinetic parameters with the heating rate can be observed ($k_{533\text{K}}$ does not change significantly). The same mechanism was found for reaction (2) in the ranges $0 < \alpha < \alpha_{ip}$ and $\alpha_{ip} < \alpha < 1$, although for $\alpha_{ip} < \alpha < 1$ the contracting cylinder mechanism gives a lower value of the mean square deviation. No induction period was apparent for reaction (2). Slight differences between the values of the pre-exponential factor A and activation energy E for $0 > \alpha < \alpha_{ip}$ with respect to the corresponding values for $0 < \alpha < 1$ can be noticed.

For reaction (3), as shown in Table 2, the most probable mechanism corresponds to a contracting cylinder, with a non-compensated change in the non-isothermal kinetic parameters with heating rate (the values of $k_{588\text{K}}$ change with the heating rate). In such conditions, due to heat transfer limitations, the non-isothermal kinetic parameters obtained at the lowest heating rate should be considered the true values.

For reaction (3), because there is no clear inflection on the TG curve, and a sharp maximum on the DTG curve, the non-isothermal kinetic parameters were not evaluated over selected conversion ranges.

CONCLUSIONS

The investigated polynuclear coordination compound decomposes to a mixture of magnetic Fe_3O_4 , ZnO and Fe_2ZnO_4 . By using discrimination methods, the most probable mechanism and the non-isothermal kinetic parameters were determined for $0 < \alpha < 1$. For $0 < \alpha < 1$, the most probable mechanisms of all three reactions investigated correspond to a contracting sphere geometry. There is a slight change in the values of the non-isothermal kinetic parameters of reaction (2) with the degree of conversion.

REFERENCES

- 1 M. Brezeanu, E. Segal, V. Mincu, L. Patron and S. Ciobanu, Brevet Romania, Nr. 77972 (1971).
- 2 M. Brezeanu, G. Dinu, E. Segal, V. Mincu and S. Ciobanu, Brevet Romania, Nr. 77973 (1971).
- 3 M. Brezeanu, E. Segal, V. Mincu, I. Jitaru and C. Mandravel, Brevet Romania, Nr. 79644 (1972).
- 4 M. Brezeanu, E. Segal, L. Patron, E. Safarica and T. Robu, Rev. Roum. Chim., 27 (1982) 137.
- 5 M. Brezeanu, E. Tatu, S. Bocai, O. Brezeanu, E. Segal and L. Patron, Thermochim. acta, 78 (1984) 351.

- 6 T. Coseac, S. Bocai, M. Brezeanu and E. Segal, *Thermochim. Acta*, 95 (1985) 2267.
- 7 M. Brezeanu, L. Patron, O. Carp, E. Cristurean, A. Antoniu, M. Andruh, A. Gheorghe and N. Stănică, *Rev. Roum. Chem.*, in press.
- 8 T. Coseac and E. Segal, *Thermochim. Acta*, 149 (1989) 189.
- 9 O. Carp and E. Segal, *Thermochim. Acta*, 185 (1991) 111.
- 10 H. Klug and L.E. Alexander (Eds.), *X-Ray Diffraction Procedure*, John Wiley, New York, 1962, p. 401.